Pro Gradu thesis:

Carbon nanotube azafullerene peapods and their electronic transport properties

Ville Kotimäki

UNIVERSITY OF JYVÄSKYLÄ
DEPARTMENT OF PHYSICS

Preface

The sample fabrication and the measurements presented in this thesis have been done at the Department of Physics and Nanoscience Center in the University of Jyväskylä from May 2007 to July 2008.

First I would like to thank my supervisor Prof. Päivi Törmä for giving me the opportunity to experience working in the fields of theoretical and experimental physics. The last three years in "ELE"-group have been interesting and I have gained a good insight on the different sides of nanophysics. I would also like to thank Dr. Andreas Johansson and PhD student Marcus Rinkiö for their teachings and advice that have helped me a lot in getting familiar with experimental work. I would also like to express my gratitude to all of the experimental ELE-group members who have offered their help whenever I got myself into trouble with laboratory work.

Many thanks to Dr. Lars Melwyn Jensen, Dr. Jami Kinnunen and PhD student Timo Koponen for giving me advice and guidance during the time I was working with ultra-cold quantum gases, computational physics and coding in general. I also thank the other members of the theoretical ELE-group.

I would like to credit departmental administrator Soili Leskinen, lecturer Juha Merikoski and the rest of the crew of the Department of Physics for maintaining the high quality and friendly learning environment during my studies. I am also very grateful for the opportunity to teach younger students, it was a great addition to my studies.

My special thanks go to Holvi for providing the fruitful working environment for my studies. I have been delighted to work among you guys.

Contents

1 Introduction

Carbon nanotubes have been one of the main subjects of research in nanophysics during the last ten years due to their interesting electronic, mechanical and chemical properties. The basics of carbon nanotubes are discussed in the second chapter. Separate sections are dedicated to future and present applications for carbon nanotubes, manufacturing processes of fullerenes and carbon nanotubes and the simple theory of electrical conductance of carbon nanotubes. A method for inserting different molecules inside carbon nanotubes is also briefly discussed.

The third chapter is dedicated to the portrayal of the manufacturing process of the measured carbon nanotube devices. In this work we measured carbon nanotube peapod based FET devices with a back gate geometry. The devices were manufactured on top of a silicon (Si) chip with an insulating layer of silicon oxide (SiO_2) between the device and the silicon back gate. Palladium (Pd) and scandium (Sc) were used to fabricate the electrodes which were used to connect the nanotube to our home made measuring setup. Different manufacturing phases, equipment and problems are explained in the third chapter.

In this work we measured the IV characteristics, electronic transfer characteristics and the ability of carbon nanotube peapods to work as a memory device by a voltage pulse measurement. All of the measured devices were found out to be p-type contrary to some earlier results from similar but not exactly alike measurements [1, 2, 3]. The hysteresis phenomenom was observed with a very small but stable on/off ratios between 1.2 to 3. The resistance of the peapod devices was measured to be between tens and thousands of kilo ohms depending on the electrode material. The oxidation of scandium was found out to be the main reason between the differences in sample resistances. The conducted measurements and the results are described in the fourth chapter of this work.

The amount of working samples was relatively few and it was clearly not sufficient for a statistical analysis. Now that we have overcome the biggest difficulties in sample fabrication process we need to continue the sample fabrication and reproduce the explained results a few more times to make more confident conclusions.

2 Carbon Nanotubes and Fullerenes

Fullerenes are molecules formed entirely of carbon and they were discovered in 1985 by Robert Curl, Harold Kroto and Richard Smalley [4]. The discovered fullerenes were the buckministerfullerenes, which are spherical carbon molecules (C_{60}) and are similar to a football with 32 faces. "Buckyball" structure consists of hexagons and pentagons which are aligned so that each pentagon is surrounded by five hexagons (see fig. 1). Fullerenes can exist in the form of a hollow sphere, ellipsoid, tube or flat sheets depending on the manufacturing process. Due to the approaching limitations in miniaturisation of silicon based computer components, carbon based nanostructures have become more and more interesting as a subject of research.

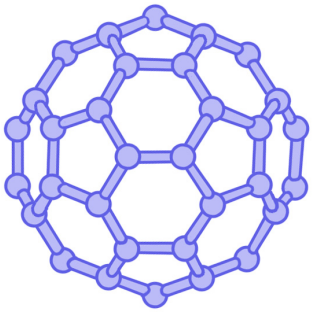

Figure 1: An illustration of a buckyball fullerene (C_{60}).

One of the most promising carbon allotropes is a tube-shaped carbon nanotube (CNT) which was discovered in 1991 by Sumio Iijima [5]. Carbon nanotubes are structures which can have length/thickness ratio as big as 10^4 making them effectively one-dimensional nano-objects. One way to imagine the CNT structure is to take either one or a few graphene sheets and fold them into a cylinder. CNT made from one graphene sheet is a single walled carbon nanotube (SWCNT) and the one made from a few sheets is a multi walled carbon nanotube (MWCNT). Usually the thickness and the length of SWCNTs can vary between $1\ \mathrm{nm}$ to $2\ \mathrm{nm}$ and $100\ \mathrm{nm}$ to $10\ \mu\mathrm{m}$

respectively. MWCNTs are as long as SWCNTs but they are thicker with diameters ranging from $2.5\ \mathrm{nm}$ to $100\ \mathrm{nm}$.

CNTs make an interesting subject for research since they posses some quite extraordinary properties for this kind of organic molecule. They are harder than diamond while being much lighter molecular structure and their conductivity is a couple orders of magnitude higher than the conductivity of silver or copper. CNTs are also chemically inert and contain relatively few defects in their wall structure. In addition to graphene, CNTs are one of the main candidates for replacing Si as a material for small electronic devices. It has been reported that CNT-based devices could be built with a component density of $10^{12}\ \mathrm{cm}^{-2}$ [6] which is approximately 4 orders of magnitude higher than with the Si-based manufacturing processes used nowadays.

2.1 Applications for carbon nanotubes

Even though this work consists mainly of discussion about the electrical properties of the carbon nanotubes, CNTs have a wide selection of other future and present applications as well. Some of the applications are short term which are expected to hit the shelves in less than ten years while others are long-term having the prospect of commercial products beyond the ten-year time frame. In this section we have a quick overview of the few fields of applications for carbon nanotubes.

One of the main topics in CNT research is their use in electronics and energy products. The SWCNTs have been used to produce p-type, n-type and bipolar transistors [7, 8, 9, 10]. It has been shown that the CNT power transistors can posses 20 times smaller switching resistance and 200 times more current-handling capability than conventional power MOSFETs. Some CNTs may also be used as an interconnect because of their ballistic electronic transport capability and metallic behaviour [9, 11]. In addition, CNTs can be used to make single molecule memory devices [12, 13], invisible circuits based on transparent transistors [14] and better insulator

plastics because they prevent the charge buildup on the surface of the insulating material [9]. CNTs can be used to make better lithium-ion batteries [15], fuel [16] and solar cells [9]. It has also been reported that CNTs have a good thermal conduction in axial direction allowing arrays of CNTs to be used as an efficient cooling solution for small electronic devices [17]. The most of the electronical applications for carbon nanotubes are considered as a long-term applications because of the problems in device manufacturing processes. Applications that do not require a precise placement of CNTs, like an insulator plastic for an example, are most likely going to be available in a five to ten years time frame.

Research has been made to use carbon fibers to reinforce high strength, light weight and high performance composites [18]. If CNTs could be utilized properly they should perform much better since they are considered as the best carbon fiber with superior mechanical properties. The progress of the research in mechanical applications of carbon nanotubes has not been advancing lately because of CNTs are atomically smooth, difficult to adhere on other materials and the load cannot be properly transfered. CNTs are also relatively short fibers and when they are produced in large amounts they come in bundles which are known to behave differently compared to single CNTs. The most probable use of CNTs might not be the primary load-bearing structure but the matrix enhancer in composite materials. CNTs are currently used as nanotube-blended plastics in superior sporting goods [9]. Other possible applications for CNTs include the damping alleviation in aerospace and automobile products [19] and the use as a microcatheter which has been studied and found to be far superior compared with a neat polymer-derived catheter [20].

The carbon nanotubes have also found to be effective as gas-sensing elements [21]. The principle of a gas sensor is to measure the electrical conduction which differs depending on the gases the CNT sensor has been exposed to. CNT based gas-sensors excel in power consumption, sensitivity, miniaturization and reliable mass production. CNT based gas-sensors

are already found on the store shelves but the research is still being done to improve the sensitivity and the selectivity. The use of CNTs in other types of sensors is also being conducted [9].

CNTs have a good emitter lifetime, good emission stability and low threshold voltage which makes them ideal field emitters. These qualities have been used for creating cathode-ray lightning elements and flatpanel displays which are based on CNTs [22]. There have been several prototypes of CNT based flat panel displays and they are likely to hit the market in the next five years.

There are also some medical applications for CNTs. Because of the optical properties of the CNTs there have been some studies regarding their use in imaging applications within live cells and tissue [23]. CNTs are also considered as a new delivery vehicles for drugs [9]. The nanotubes have higher surface area to volume ratio than spheres which makes them better at delivering therapeutic agents. There are still quite many issues to solve, making the CNTs soluble to liquid organic media and the functionality of cargo unloading process for an example. The toxic properties of CNTs are still not properly known making CNTs effectively unusable in medical treatments. Because of the amount of research that needs to be done, biological and medical applications are considered as a long-term project.

2.2 Manufacturing of carbon nanostructures

Nowadays there are several different methods for making CNTs and fullerenes. Fullerenes were originally found after using a short-pulse, high-power laser to vaporize graphite [4]. The technique utilized by Curl, Kroto and Smalley was not suitable for producing carbon nanostructures in large amounts. It is suspected that CNTs are not new carbon nanostructures. They have probably been made by using different carbon combustion and vapor deposition processess several years ago but they have not been observed because of the lack of a proper microscope technology.

The first method for producing carbon nanostructures in reasonable

amounts was arc discharge method (ADM). The basic principles of ADM and three other methods are explained in the following four sections.

2.2.1 Arc Discharge Method

The carbon arc discharge method (ADM) was first used for producing C_{60} fullerenes and it is regarded as the easiest way to produce large quantities of CNTs. The downside of the method is that it requires more processing and purification because it produces a complicated mixture of nanotubes and residual catalytic metals.

The ADM is used by situating two carbon rods end to end so that there is a small gap in between them. After this the gap is filled with an inert gas at low pressure followed by applying a potential difference between the rods. This will cause a direct current between the rods thus producing a high temperature discharge between the two electrodes. The discharge vaporizes the surface of the first carbon electrode, and forms a small rod-shaped deposit on the other electrode. Production of CNTs depends on the operation temperature and the quality of the plasma arc. The fullerenes can be found from the formed soot and MWCNTs and SWCNTs [24] from the opposing electrode. An illustrative image of the ADM setup can be seen in figure 2. [25]

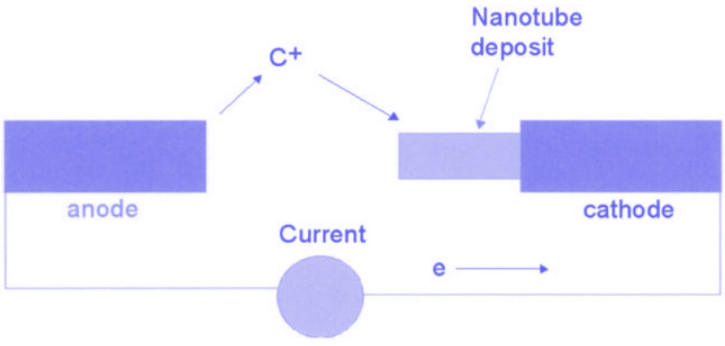

Figure 2: An illustration of ADM setup [25].

2.2.2 Laser Vaporization Method

Lazer vaporiation method (LVM) has been used to produce CNTs since 1996. Dual-pulsed laser is used to vaporize graphite rods with a 1:1 catalyst mixture of cobalt and nickel at $1200\ ^{\circ}\mathrm{C}$ in flowing inert gas. C_{60} and other unwanted fullerenes are removed by giving a $1000\ ^{\circ}\mathrm{C}$ heat treatment in vacuum. Dual-pulsing is used to achieve more uniform vaporization and to minimize the amount of carbon deposited as soot. Larger particles which are ablated by the first pulse are broken by the second pulse and fed into the growing nanotube structure.

LVM is a carbon vaporization technique just like ADM so it possesses the same drawbacks of nanotube growth. Nanotubes appear in highly tangled forms, mixed with unwanted forms of carbon and/or metal. The CNTs aligned along a common axis form a carpet of "ropes" which are approximately $100\ \mu\mathrm{m}$ long and have a thickness between 10 to $20\ \mathrm{nm}$. This method produces mainly SWCNTs in a bundled rope-like structure. The average CNT diameter and size distribution can be varied by modifying the growth temperature, the catalyst composition and other process parameters. [25]. It has been shown that this manufacturing method produces small amounts of CNTs which have C_{60} fullerenes trapped inside [26].

2.2.3 Chemical Vapor Deposition

One of the oldest methods of producing varied carbon materials such as carbon fibers and filaments is chemical vapor deposition (CVD) of hydrocarbons over a metal catalyst. Desired deposit is grown on top of the selected substrate by exposing the substrate to one or more volatile precursors which react and/or decompose on top of the substrate. The gas is kept flowing through the reaction chamber to ensure the removal of the unwanted volatile by-products which are frequently produced during the CVD-process. CVD can be used to produce large amounts of CNTs with

relatively high defect densities [27].

Catalytic CVD of acetylene over cobalt and iron catalysts supported on silica or zeolite can be used to form large amounts of CNTs. The variety of CNTs seems to be dependant on pH value in catalyst prepration while the deposition activity is related to the cobalt percentage of the catalyst. CVD with carbon/zeolite catalyst was found to produce fullerenes and MWCNTs in addition to SWCNTs. Catalytic decomposition of an H_2/CH_4 mixture over spread out metal particles such as cobalt, nickel and iron on magnesium oxide at $1000\ ^\circ\mathrm{C}$ has been perceived to produce large amount of SWCNTs.

Selective reduction of oxide solid solutions between a non-reducible oxide such as Al_2O_3 or $MgAl_2O_4$ and one or more transition metal oxide(s) in H_2/CH_4 atmosphere can be used to obtain composite powders containing well-spread CNTs. The reduction generates transition metal nanoparticles at a temperature of regularly $>800\ ^\circ\mathrm{C}$. The growth of the new nanoparticles is prevented by the decomposition of CH_4 resulting in a very high SWCNT/MWCNT ratio. [25].

2.2.4 Ball Milling

Ball milling (BM) followed by annealing is a relatively new way to produce CNTs. The method has been used to create different kinds of porous nanoscale microstructures but it was harnessed to the production of CNTs just a few years ago. The method consists of three steps: First, the graphite powder and four hardened steel balls are put into a container made of stainless steel. After that the container is purged and the milling takes place at room temperature for up to 150 hours while argon is brought into the system. The final step of this process is nitrogen (or argon) gas flow annealing at temperatures of $1400\ ^\circ\mathrm{C}$ for six hours.

Even though the principle of this process is not known it is thought that the nanotube nuclei is formed by ball milling process and the nanotube growth is activated by the annealing. It has been shown that the

main product of this process are MWCNTs while SWCNTs are the definite minority. [25].

2.3 CNT Peapod fabrication

People have been keen on researching different ways to alter the electrical and the mechanical properties of the CNTs. Because the pristine CNTs are hollow cylinder shaped nanostructures the most natural choice to modify their properties is to try to get atoms or molecules inside the CNTs [1]. The laser vaporization method is known to produce C_{60} filled CNTs, but the amount of peapods is so small that a specific process is required for the CNT peapod production.

One of the ways for getting fullerenes inside the CNTs is heating. First, the fullerenes were created by using the arc discharge method and isolated with the use of multistage high-performance liquid chromatography technique. The CNTs were manufactured with the laser vaporization method and cleaned with an acid treatment for $8\ \mathrm{h}$ at $160\ ^{\circ}\mathrm{C}$. After cleaning the CNTs were heated in dry air for $20\ \mathrm{min}$ at $450\ ^{\circ}\mathrm{C}$ to open the tube ends. Finally, the prepared CNTs and fullerenes were put into a sealed glass ampule and the doping was carried out by heating the ampule at $500\ ^{\circ}\mathrm{C}$ for $24\ \mathrm{h}$. [28]

It was suggested that the acid treatment in the sample processing phase breaks CNTs by making small hole defects for fullerenes to slip in [29]. This was proven wrong later by Iijima *et al.* [28]. They showed that it is possible to create CNT peapods withouth chemical cleaning.

The pristine fullerenes can be modified to contain some foreign atoms inside. The other way to modify the electronic structure of the fullerenes is to replace some carbon atoms with other atoms, nitrogen for an example [1].

[1] A carbon nanotube containing molecules within it's structure is called a peapod.

2.4 Electrical properties of carbon nanotubes

Earlier in this chapter we described carbon nanotubes as a folded sheet of graphene. It has been shown that the electrical properties of a SWCNT depend heavily on the way the graphene sheet is folded. Because of the shape of honeycomb lattice of the graphene sheet the SWCNT's geometry can be completely specified with a pair of integers (n, m). The relative positions of two "combs" in the honeycomb lattice can be defined with the use of chiral vector

$$\mathbf{C} = n\mathbf{a}_1 + m\mathbf{a}_2, \tag{1}$$

where the primitive translation vectors of the honeycomb lattice are defined

$$\begin{aligned} \mathbf{a}_1 &= a\left(\frac{\sqrt{3}}{2}\mathbf{x} + \frac{1}{2}\mathbf{y}\right) \\ \mathbf{a}_2 &= a\left(\frac{\sqrt{3}}{2}\mathbf{x} - \frac{1}{2}\mathbf{y}\right), \end{aligned}$$

where the length a can be expressed with the carbon-carbon (C-C) bond length $a_{C-C} = 0.144nm$

$$a = \sqrt{3}a_{C-C}. \tag{2}$$

The chiral vector can be used to construct a SWCNT by folding the graphene sheet along the direction given by $\mathbf{C}$ as explained in figure 3.

The circumferencial length of the formed nanotube is

$$|\mathbf{C}| = \pi d = \sqrt{3}a_{C-C}\left(m^2 + mn + n^2\right)^{1/2}, \tag{3}$$

where d is the diameter of SWCNT. The angle of chirality is defined to be the angle between $\mathbf{C}$ and $\mathbf{a}_1$ and it can be expressed with the use of the two integers n and m and has the form

$$\tan\theta = \frac{\sqrt{3}m}{2n + m}. \tag{4}$$

Because of the symmetry properties of graphene sheets three types of SWCNTs can be produced by folding the sheet as explained above. Three types

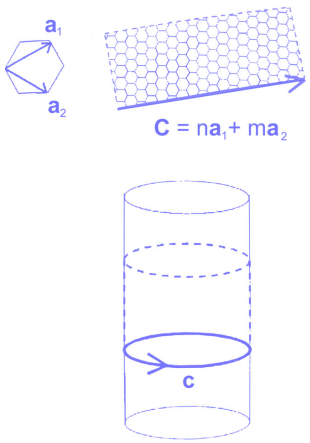

Figure 3: An illustration of SWCNT folding [27].

are named zigzag $(n, 0)$, armchair (n, n) and chiral nanotubes with the angle of chirality $\theta = 0°$, $\theta = 30°$ and $0° < \theta < 30°$ respectively. Figures 4 and 5 show some of the possible vectors specified by the pairs of integers (n, m) and the schematic models for SWCNTs with nanotube axis normal to the chiral vector respectively. [27]

It has been shown that the electrical properties of CNTs depend strongly on their geometric structure. The CNTs can be be either metals or semiconductors with different size energy gaps depending on the diameter and the helicity of the CNTs. Theoretical calculations have shown that the nature of a certain SWCNT can be calculated from the diameter and the helicity of the tube, i.e., on the indices (n, m). There are three general rules for the metallicity of the SWCNT: armchair (n, n) CNTs are metals; (n, m) tubes with $n - m = 3j$, where j is a non-zero integer, are semiconductors with a very small energy gap; and all others are semiconductors with large energy gaps. [27, 30]

Because carbon nanotubes can be considered as wrapped graphene sheets the electrical properties of CNTs can be deduced from the characteristics of a single graphene sheet. The extraordinary electronic properties of the CNTs arise from the one-dimensional nature of their structure. Elec-

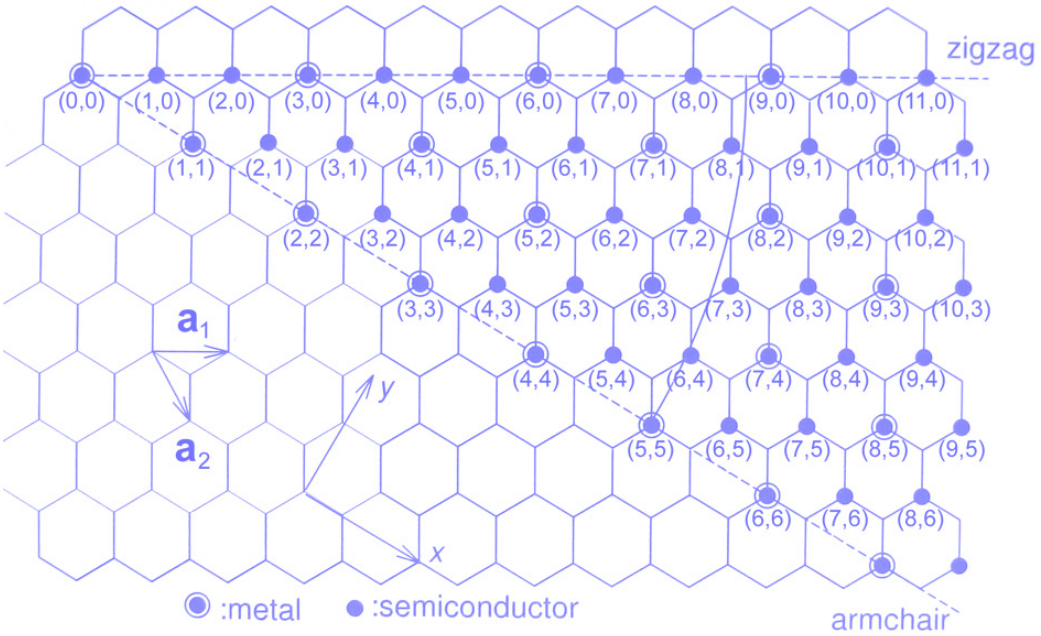

Figure 4: Possible vectors specified by the two integers (n, m) for the three types of CNTs. (n, n)-line corresponds to armchair nanotubes while $(n, 0)$ - line is for zigzag nanotubes leaving chiral nanotubes in between them [27]. The rought electrical properties of a certain SWCNT is represented with a dot or an encircled dot. Metallic SWCNTs (n, n) and semiconducting SWCNTs with a small energy gap ($n - m = 3j, j \in \mathbb{Z}\backslash\{0\}$) are portrayed by encircled dots and large gap semiconductors are portrayed by regular dots.

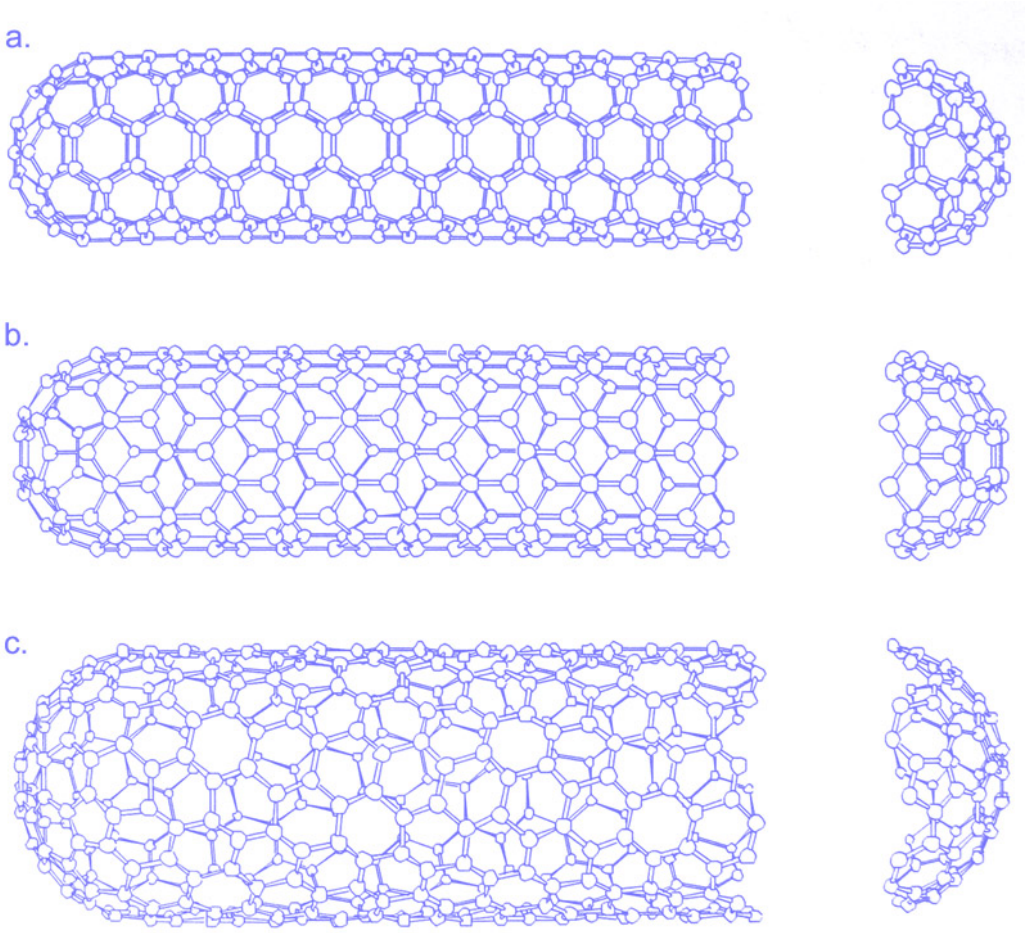

Figure 5: Schematic models of (a.) armchair SWCNT $(5, 5)$, (b.) zigzag SWCNT $(9, 0)$ and (c.) chiral SWCNT $(10, 5)$ [27].

trons are confided inside CNT and can only move in the direction of the tube axis. This, energy and momentum conservation together cause a reduced "phase space" for scattering processes thus allowing larger current densities than in metals such as Al or Cu. [30]

The theoretical maximum of the electrical conduction of a SWCNT can be found if the scattering is totally neglected and the electron transport is completely ballistic. Using the Landauer's equation one can obtain the maximum conductance $G_{max} = 4e^2/h =: G_0$ which corresponds a resistance of $6.5\ \mathrm{k}\Omega$. This is the quantum mechanical contact resistance caused by the incongruity of the number of conduction channels in the CNT and the metal electrodes which are used to connect the CNT to the device. This is only one part of the total resitance of the device, poor coupling between the CNT and the leads and Schottky barriers at metal- and semiconductor-CNT junctions are also important sources of the final device resistance. [30]

The sensitive dependance of electrical properties on the diameter and wrapping angle (integers (n, m)) of SWCNT has been verified experimentally. Scanning tunnelling microscopy [31] and resonant raman scattering [32] have been successfully used to determine the structure of measured SWCNTs.

2.4.1 Modification of the band structure

The semiconducting behaviour of CNTs was first reported by Tans *et al.* in 1998 [7]. A field effect transistor was made by connecting a semiconducting carbon nanotube with two metal electrodes. The nonlinearity of the device was found by adding a voltage to a gate electrode. The gate electrode produced an electric field which was used to change the conductance of the device. Most of the semiconducting CNTs[2] work like p-type FETs because their conductance gets bigger when a negative gate voltage is applied. There have also been reports of CNTs which have shown both

[2]Hence the acronym "CNT" refers to a semiconducting carbon nanotube

p- and n-type behaviour by displaying increase in electrical conductance with both negative and positive gate voltages. This ambipolar behaviour is more common to carbon nanotubes with a relatively large diameter [10].

The mechanism for the FET-like behaviour of CNT devices is not yet fully understood but there are two proposed models which are equally supported. The first model suggests that carbon nanotubes work exactly like regular semiconductors. The external electric field modulates the valence and the conduction bands thus allowing easier excitation of electrons within the nanotube band structure. This will increase the conductance of the carbon nanotube device. The other model states that modulation of the band structure of the carbon nanotube is not the main mechanism in controlling the conductance. Instead it is suggested that the Schottky barriers at the CNT-metal contacts play a central role when the conductance of CNT device is determined [33]. In this case the external electric field controls the width of the barrier. The conductance of CNT device is increased when the barrier is narrowed to allow more electron tunneling through the CNT-metal contact. The size of Schottky barrier can also be decreased by selecting a suitable electrode material which in the best cases can produce ohmic contacts to the CNT [34, 35].

2.4.2 Hysteresis effect

The CNT devices operate very similarly to regular Si based FETs. Some of the challenges of Si based manufacturing processes are also visible in CNT based electronic devices. Just like Si FETs some CNTFETs have the ability to remember the history of the applied electric field. The states of these CNT devices cannot be predicted from the current parameters but the history of the devices must be taken into account. The conductance of the CNT devices depend on the alignment and strength of a local electric field previously induced by the gate voltage thus producing this hysteresis effect [12]. Unlike manufacturing processes for CNT based electronics, those for Si devices have already evolved to a state where hysteresis phe-

nomenon can be controlled.

The origin of the hysteresis phenomenon is believed to be related to charge traps located in the vicinity of the device. When the electric field is applied the band structure changes and the tunneling probablity of charge carriers is increased. The larger the electric field the more charge carriers are tunneling into the charge traps. This change in the charge distribution produces local electric field with a screening effect inside the device. The screening effect alters the electric field "felt" by the device and changes the band structure accordingly making the electrical conductance dependent on the amount of trapped charge carriers. If the electric field is tuned down to zero some of the charge carriers are still trapped and the conductance of the device differs from the situation before adding the electric field even though the electric field is removed. Freeing the charge carriers requires an electric field directed to the opposite direction in relation to the field used before.

The mechanism for hysteresis is not yet fully understood but there are four proposals for solving the problem. The first of the models does not actually involve charge trapping but the movement of mobile charge in the SiO_2 surface [12]. If the mobile charge within the SiO_2 would relocate because of the electric field caused by the gate electrode it would cause a distortion in the local electric field inside the CNT, hence producing the hysteresis effect explained in the previous paragraph. Two other possible explanations of the charge trapping are that there might be charge traps on the surface of the SiO_2 layer [12, 36] or the charge can be trapped in the water molecules attached to the SiO_2 surface [37]. The fourth model suggests that defects on the surface of the CNT could provide charging centers which can vacate or accept electrons to or from the conduction channel [13, 38, 39]. Any of these mechanisms are not exclusive and they may all contribute to the total charging effect seen in the CNT device measurements.

3 Sample fabrication

The whole sample fabrication process was done in ISO Class: 6-5 (1000-100) cleanroom except for atomic force microscope imaging and bonding.

3.1 Base chip for CNT deposition

The first step in sample preparation is the fabrication of the chip which is used as a base for the CNT samples. The material used here was a SiO_2 covered Si chip. A plain Si wafer was oxidized in a Carbolite oven at $1100\ ^{\circ}\mathrm{C}$ for 5 hours to get a roughly $300\ \mathrm{nm}$ thick SiO_2 layer on top of the Si chip.

The second step in preparing the base chip for CNT deposition was the first electron beam lithography run. Electron beam lithography was used to draw the first electrode structure on the chip. In addition to the first electrode structure the electron beam lithography was also used to draw an inner marker structure which was used in the positioning of CNTs. The inner electrode and marker structures are illustrated in figure 6.

The electron beam drawing can be divided into two phases. First, one must spin a thin resist layer on top of the chip. In this work the resist layer consisted of two different resists. The first resist layer was made of polymethyl methacrylate dissolved in anisole (PMMA 495 A3). The chip was spun at $3000\ \mathrm{r/min}$ for 50 seconds with a BIDTEC SP100 spinner while the resist was put on top of the chip with a dropper. After spinning the resist was baked by putting the chip on top of a heating plate at $160\ ^{\circ}\mathrm{C}$ for 3 minutes, resulting in an approximately $100\ \mathrm{nm}$ thick resist layer. Baking must be done to solidify the resist, and thus allow further processing. The second resist layer was approximately $60\ \mathrm{nm}$ thick and was made off polymethylmethacrylate dissolved in anisole (PMMA 950 A2). The spinner speed was $6000\ \mathrm{r/min}$ and the baking time and temperature were the same as before. Two resists were used because the first resist is more prone to dissolve when embed to a suitable developer solution. This was done

because it will lead to a profitable undercut structure for the lift-off phase, as illustrated in figure 7.

After the resist layers were prepared, electron beam lithography was used to draw electrodes and the inner marker structure on top of the resists. Electron beam affects the resist layers so that only the exposed part will become vulnerable to a developer solution while the unexposed parts are not affected by developing. The electron beam lithography was done with a Raith e-line electron-beam writer. The e-line writer was controlled with an Elphy Quantum 4.0 SP 8.0 -lithography software. The patterning was done with acceleration voltage of $20\ \mathrm{kV}$ and area dose of $220\ \mu\mathrm{As/m^2}$. Because of the structure of the base chip, two working areas (WA) were used with different aperture sizes. Outer structure was processed with $2500\ \mu\mathrm{m}$ WA and $120\ \mu\mathrm{m}$ aperture size and inner structure with $500\ \mu\mathrm{m}$ WA and $30\ \mu\mathrm{m}$ aperture size. The chip was embedded into a developer solution to finalize the resist mask for evaporation. We kept the chip in 1:3 methyl isobutyl ketone:isopropyl alcohol (MIBK:IPA) solution for 60 seconds to get rid off all exposed parts of the resist. After removing the exposed parts the chip was washed with IPA and dried with nitrogen flow.

Before proceeding to the evaporation phase the masked chip was cleaned with reactive ion etching (RIE). The procedure was carried out by using an Oxford Instruments Plasmalab80Plus reactive ion etcher and the chip was treated with 20 seconds of oxide plasma at a power of $28\ \mathrm{W}$. RIE was used to remove possible residues or remaining monolayers of resist from the surface of the chip. It also removes a few monolayers from the mask of resist, but that has of course a negligible effect on the liftoff.

We did the electrode evaporation with a Balzers BAL-TEC BAE250 Coating System and used palladium and titanium as evaporation materials. The evaporation crucibles made of graphite were heated with a focused electron beam. We started with titanium and evaporated $5\ \mathrm{nm}$ layer with evaporation rate of $0.07\ \mathrm{nm/s}$. Titanium was used to ensure a good adhesion for the palladium electrodes which were evaporated after tita-

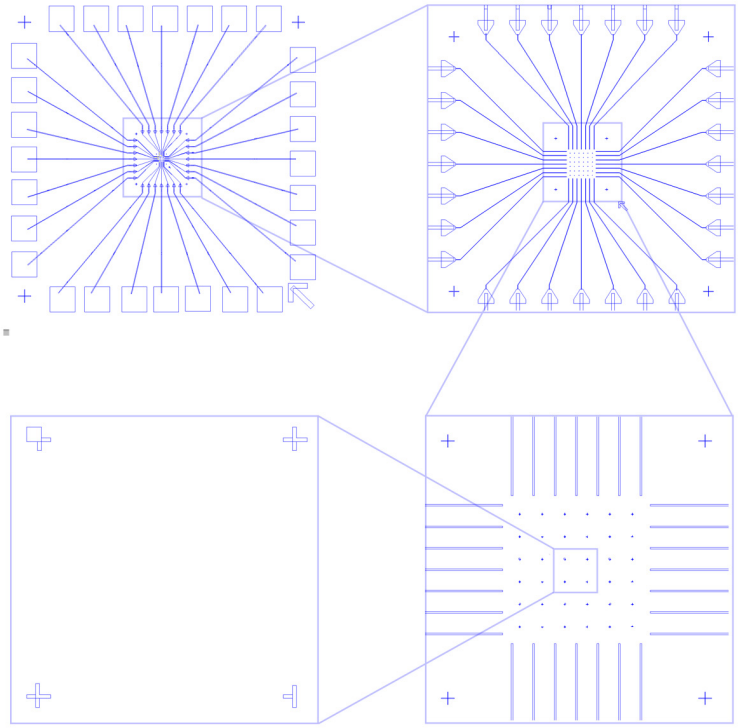

Figure 6: Magnified electrode structure on top of the base chip.

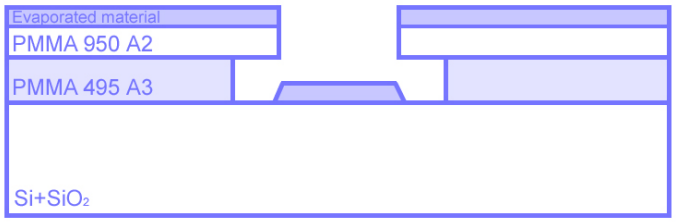

Figure 7: An illustration of the double layer undercut structure after the evaporation.

nium. The amount of evaporated palladium was $25\ \mathrm{nm}$ and we used the same evaporation rate as with titanium. Evaporation of the both materials was carried out in $10^{-6}\ \mathrm{mbar}$ vacuum.

The base chip was finalized by doing a lift-off procedure. The chip was embedded in acetone immediately after the evaporation. Acetone was used to dissolve the resist under evaporated material thus leaving only the desired electrodes and marker structure on top of the chip. The undercut is made to ensure the evaporated material that is going to be removed is not connected to the pattern that should stay. The dissolving effect of acetone can be accelerated by heating and spraying acetone towards the surface with a syringe. After the lift-off the chip was washed with IPA and dried with a nitrogen flow.

3.2 SWCNT Peapod deposition and AFM mapping

The SWCNTs used in this work were filled with azafullerene dimers $(C_{59}N)_2$. The peapods were provided by N. Tagmatarchis and his group at the Theoretical and Physical Chemistry Institute, Athens, Greece. Illustration of an azafullerene dimer can be seen in figure 8.

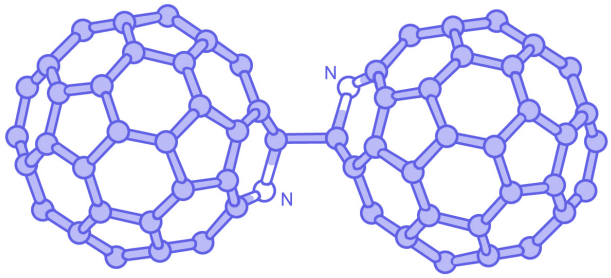

Figure 8: An illustration showing a biazafullerene structure $(C_{59}n)_2$ [40]. Biazafullerene is the stable form of the azafullerene molecule.

Small amount of SWCNT peapod powder was put into $1,2$-dichloroethane for easier deposition. The nanotube solution was sonicated with a Hielscher Ultrasound Techonology UP400S finger sonicator for 1 to 2 hours to get nanotubes separated from each other. After sonication, a couple of droplets of nanotube solution were deposited on top of a rotating (1500 rpm) base chip. The chip was rotated to ensure that there would not be any big debris on top of the chip.

The following step was to take images of the surface with an atomic force microscope (AFM). The NanoScope IV AFM with NanoScope 6.13R1(R) software was used to map the positions of the nanotubes instead of scanning electron microscope to minimize the risk of damaging the nanotubes. The marker structure was used to determine the exact position of the CNT Peapods. One of the AFM map images can be seen in figure 9.

3.3 Nanotube contact electrodes

After we were finished with the mapping of the nanotubes, a new set of electrodes was designed to connect the base chip structure with the deposited nanotubes. An example of the designed electrode structure can be seen in figure 10. The new set of electrodes was made on top of the base chip similarly to the first set of electrodes, evaporation phase being the only difference between two manufacturing steps.

We made source and drain electrodes from two different materials. Palladium electrodes were evaporated similarly to the first palladium evaporation without titanium. The other evaporation material, scandium, was more demanding. The problem with scandium is that it oxidizes easily and the scandium oxide, Si_2O_3, layer on the surface of scandium can be 20 nm to 30 nm thick [41]. If scandium is evaporated similarly as palladium, the first layer that makes contact with the base chip and the deposited Peapod CNTs will be an insulating layer of Si_2O_3.

To prevent this we must heat the scandium to remove the Sc_2O_3 layer from the surface of scandium pieces in our evaporation crucible. This was

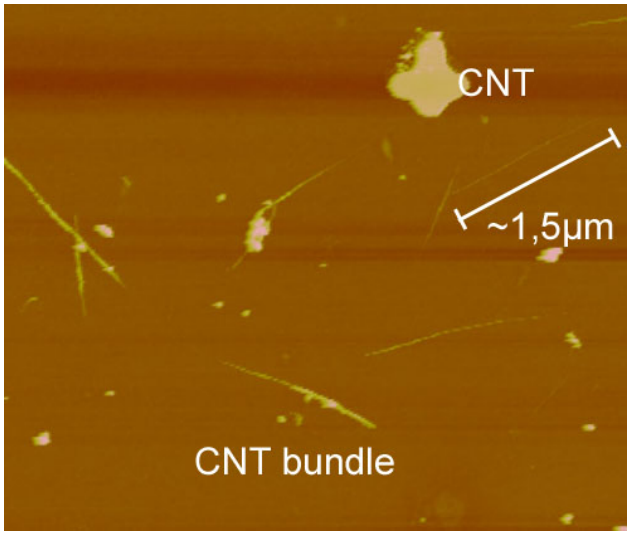

Figure 9: AFM image of nanotubes and nanotube bundles.

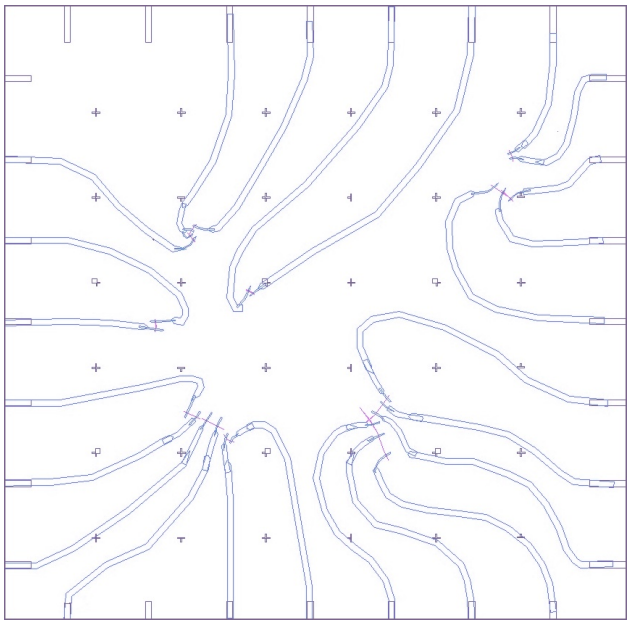

Figure 10: The contact electrode design of the sample AFP02.

done by starting the scandium evaporation with the shutter closed and evaporating $60\ \mathrm{nm}$ before opening the shutter and starting the deposition onto the sample. The oxidation is also the reason why we made the scandium electrodes twice as thick as the electrodes made of palladium.One of the finished devices can be seen in figure 11. The other possible problem with scandium was that the used heating crucibles were made of graphite and in certain circumstances scandium and graphite can form scandium-graphite which is known to be an insulator. The latter problem seemed to be the smaller of the two since we were able to produce scandium wires with relatively good conductance by using the method described before.

The lift-off procedure was carried out exactly like before and after that the sample was imaged with the AFM one more time to inspect the condition of the produced nanotube samples. An example of the finished CNT Peapod device can be seen in the figure 11. The last step of the sample fabrication was the bonding. The small chips must be bonded to chip carriers (see figure 12) which may be connected to the measuring setup. An ultra-sonic bonder was used to bond chips to chip carriers with a thin Au-wire. Two of the bonded wires were not connected to CNT Peapods but the Si layer of the base chip. This was done by connecting the respective bonding pads to the back side of the chip with silver paint.

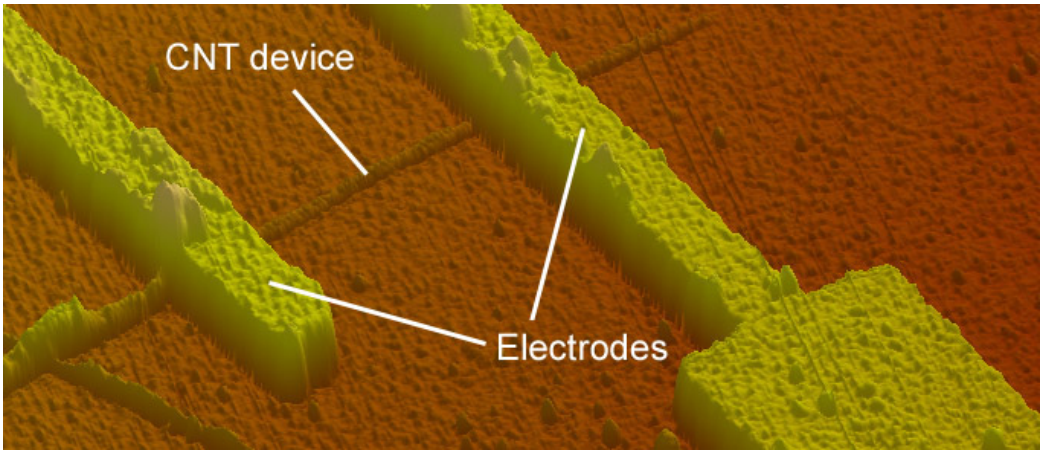

Figure 11: AFM image of a completed CNT device

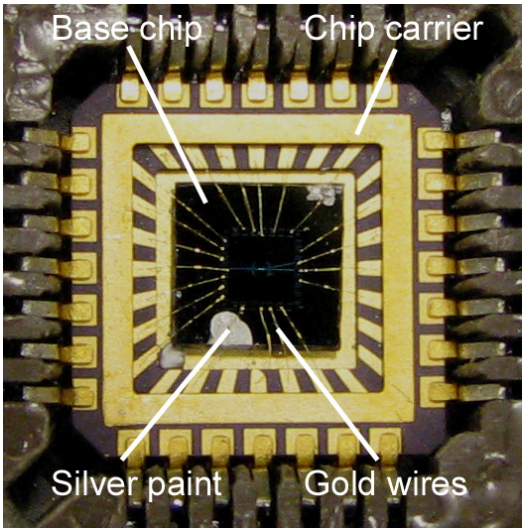

Figure 12: The bonded base chip in the chip carrier.

4 Measurements and results

4.1 Measurement setup

All measurements presented in this chapter were made in an electronically shielded room. The carbon nanotube devices were measured at room-temperature ($22\ ^{\circ}\mathrm{C}$) and $22\ \%$ relative humidity. The whole measuring setup is presented in figure 13 and the schematic circuit diagram in figure 14.

First the chip carrier was mounted into the custom built measuring box. Three of the 28 bnc connectors were attached to the measuring setup to connect source, drain and gate electrodes to our measuring setup. The source and the gate electrodes were connected to a home built voltage box. The voltage box was connected to a computer with optical lines to ensure good functionality of the voltage box.

The SWCNT peapods and the gate were connected to two low noise voltage preamplifiers and one low noise current preamplifier to amplify the measured signal to an easily measurable scale. The gate and the source-drain voltages were amplified with a Stanford Research Systems Model SR560 low-noise preamplifier and a DL Instruments Model-1201 preamplifier respectively. The source-drain current was amplified with a DL Instruments Model-1211 preamplifier. All three amplifiers were connected to the same computer through a low pass filter with a $25\ \mathrm{kHz}$ cutoff frequency, a shielded National instruments BNC-2110 connector block and a National Instruments PCI-6281 data acquisition card. To get rid of possible AC noise from a socket and ensure a pure DC-voltage measurement we used either internal or external batteries to power the voltage box and the preamplifiers.

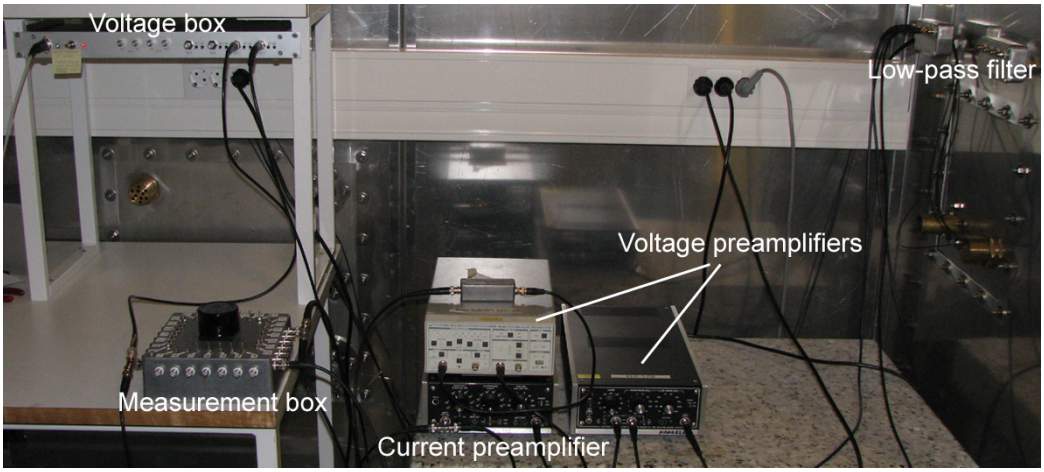

Figure 13: Measurement setup.

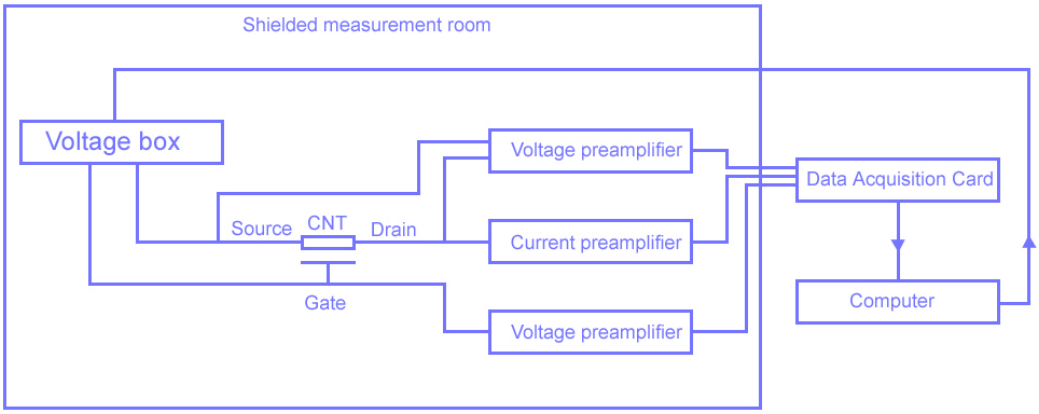

Figure 14: Schematic circuit diagram of the measurement setup.

4.2 I-V characteristics

The first step in examining CNT peapods was the measurement of the current-voltage characteristics of each peapod. The source and the drain electrodes were connected to the voltage box, the voltage preamplifier and the current preamplifier. The voltage preamplifier was used to measure voltage drop between the source and the drain electrodes while the current preamplifier was used to record the current which flowed through the SWCNTs.

All of the measured nanotubes exhibited linear response to the source-drain voltage V_{sd}. One example of the ohmic response can be seen in figure 15. The SWCNT peapods measured here were later found out to be semiconducting. The semiconducting nature of the peapods did not show up here because all of the measured devices had relatively small energy gaps. All measurements were made at room temperature which caused enough thermal excitations to make SWCNTs look ohmic and hide the semiconducting nature of the peapods.

The peapods connected with Pd electrodes had an ohmic resistance of the magnitude of $10\ \mathrm{k\Omega}$ to $100\ \mathrm{k\Omega}$ while the ones connected with Sc electrodes had ohmic resistance somewhere near $10\ \mathrm{M\Omega}$.

4.3 Carbon nanotube field-effect transistor

A field-effect transistor (FET) is a good example of a possible future application of semiconducting pristine CNTs. It is known that the electrical conductance of the CNT can be modified by varying the gate voltage of the device [7, 8]. The two different measurements used to determine the gate dependence of a SWCNT peapod device are described in the following two sections.

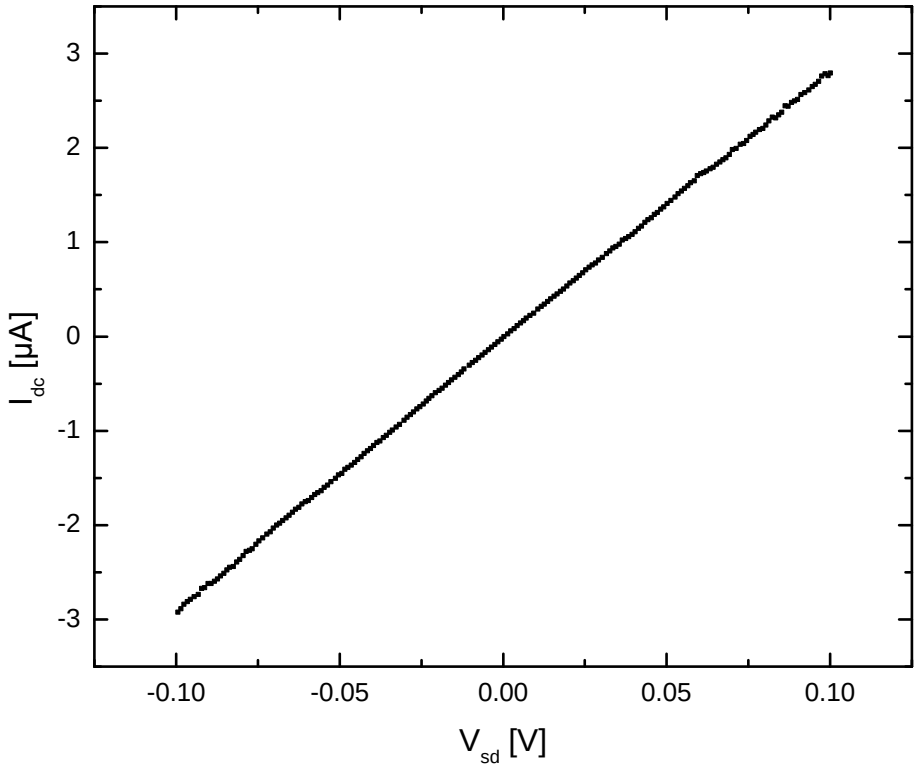

Figure 15: IV-curve of the sample AFP03NT02.

4.3.1 Transfer characteristics

After verifying that the nanotube sample was conducting with the IV-characteristics measurement we started to measure gate voltage dependence of electrical conductance of SWCNTs. The local electric field was varied by changing the back gate voltage while keeping the source drain voltage constant. The CNT is semiconducting if the electrical conductance has some gate dependance and metallic if the gate voltage does not have any effect at all.

Results for two samples with electrodes made of palladium and scandium can be seen in figures 16 and 17 respectively. The conductance of the nanotubes did not change much when we increased the gate voltage from zero to our scanning limit. Immediately after that the gate voltage was lowered to the lower limit. During lowering, the conductance of our samples started to increase. The rate of increase was lower near the upper limit of our voltage scan and higher near zero gate voltage until it decreased again near the lower limit of gate voltage. The decrease in the rate of conductance increase was not so visible with samples made with scandium electrodes. After reaching the lower limit of the voltage scan we started to increase the gate voltage. The conductance did not follow the previous curve when different scanning direction was used. The conductances of our samples were always lower with the same parameters when the gate voltage was increased.

The voltage limits ($V_G \in [-10V, 10V]$) for the samples with Sc-electrodes were higher because the change in conductance could not be seen with the lower gate voltage limits ($V_G \in [-2V, 2V]$) used with Pd contacts. The voltage limits were cautiously increased to make the gate dependence of the conductance more visible. The gate voltage scanning was immediately stopped when a leakage current was visible to prevent the samples from breaking.

The resulting curve from the conductance measurement was always a closed loop when the scanning of the gate voltage was not paused in either

end of the scanning range. If the scanning stops at the other end of the range a discontinuation can be seen in the resulting curve. This is because the time constant of the charging of SWCNT device is relatively small. When the electric field is kept constant, the amount of charge increases in the device resulting different value for the conductance when the scanning is continued.

Both of the devices opened up with negative gate voltage exhibiting p-type behaviour and the sample connected with palladium electrodes had a conductance value of approximately 10^{-1} G_0 ($G_0 = \frac{4e^2}{h}$) which was two orders of magnitude higher than the conductance value 10^{-3} G_0 of the sample connected with scandium. The resistance of the samples made with scandium was probably higher because of the oxidation effect in scandium electrodes and/or the incompatibility of scandium and the graphite crucibles which were used in the evaporation phase of sample fabrication.

The conductance is higher after turning the gate voltage down to zero from a positive value and the behaviour of the samples is the same with both electrode materials. This is an engrossing result since there have been measurements which show that behaviour of pristine carbon nanotubes changes from p-type to n-type when the electrode material is changed from palladium to scandium [2, 3]. The electron work functions of palladium (5.12 eV) and scandium (3.5 eV) differ by a few electron volts but according to our results the azafullerenes inside the SWCNTs cancel this effect. We have measured this effect with two devices with scandium electrodes and that is why more measurements are needed to make further conclusions about the effect of the dimers.

A similar measurement to ours was done in November 2007 by Hatakeyama *et al.* [1]. They measured pristine SWCNTs, buckyball fullerene (C_{60}) filled SWCNT peapods and azafullerene ($C_{59}N$) filled SWCNT peapods. The measured SWCNTs were connected with electrodes made of gold. According to their results the SWCNTs preserve their p-type transfer characteristics even if they are filled with buckyball peapods. On the other hand,

if the nanotubes are filled with azafullerenes their transport characteristics convert into n-type. They suggest that this is because azafullerenes are known by their electron donor behaviour which can modify the electronic structure of SWCNTs. The latter result is in clear contrast to our measurements. According to our results the SWCNTs retain their p-type behaviour when they are filled with azafullerenes and connected with palladium or scandium electrodes. What makes this difference so interesting is the fact that palladium and gold have similar work functions $5.12\ \mathrm{eV}$ and $5.1\ \mathrm{eV}$ respectively so that discrepancy due to the differences in work functions can be ruled out.

Another interesting part in our gate scan graphs is that both of them contain a clear sign of hysteresis phenomenon since the value of conductance at zero gate voltage depends on the previous values of the gate voltage so that the hysteresis, possibly caused by trapped charge carriers, can be seen clearly from our results.

The hysteresis effect seen in our samples is an undesirable property for a FET. FETs are required to be reliable and they are supposed to give a certain value for conductance when a particular gate voltage is applied. Because the CNTs are otherwise good candidates for replacing regular Si based components there has been interest in removing the hysteresis effect [42]. While the hysteresis effect prevents the CNT devices from being used as a FET it makes them suitable for another application which is described in the following section.

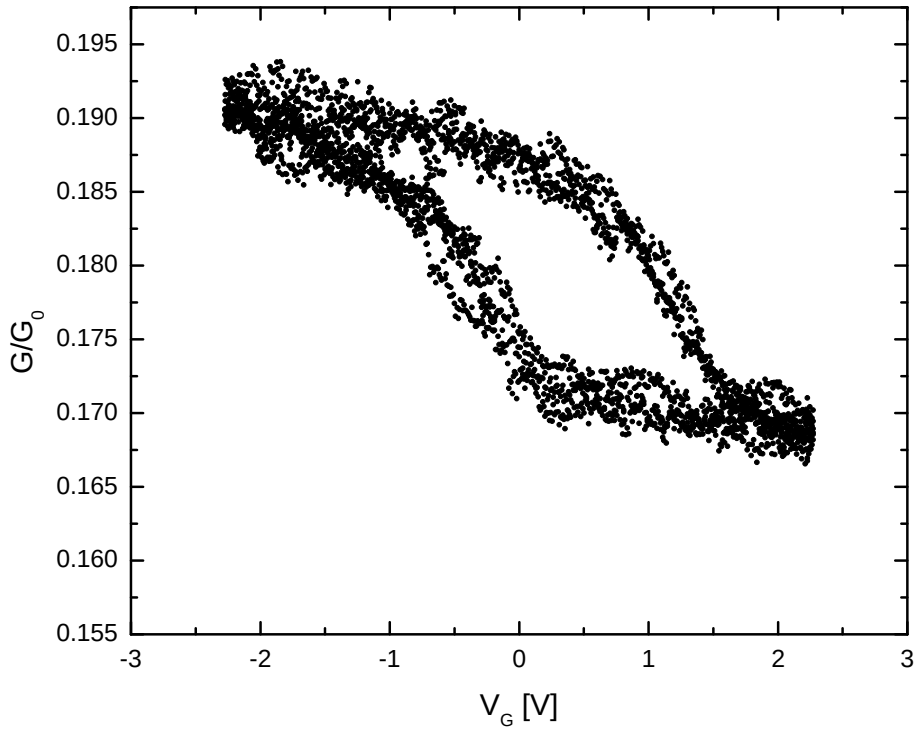

Figure 16: The conductance of the sample AFP03NT02 with Palladium electrodes as a function of the gate voltage V_G. $V_{sd} = 10.3mV, G_0 = 4e^2/h$. The direction of the gate scanning in the measurement was counter clockwise in this graph.

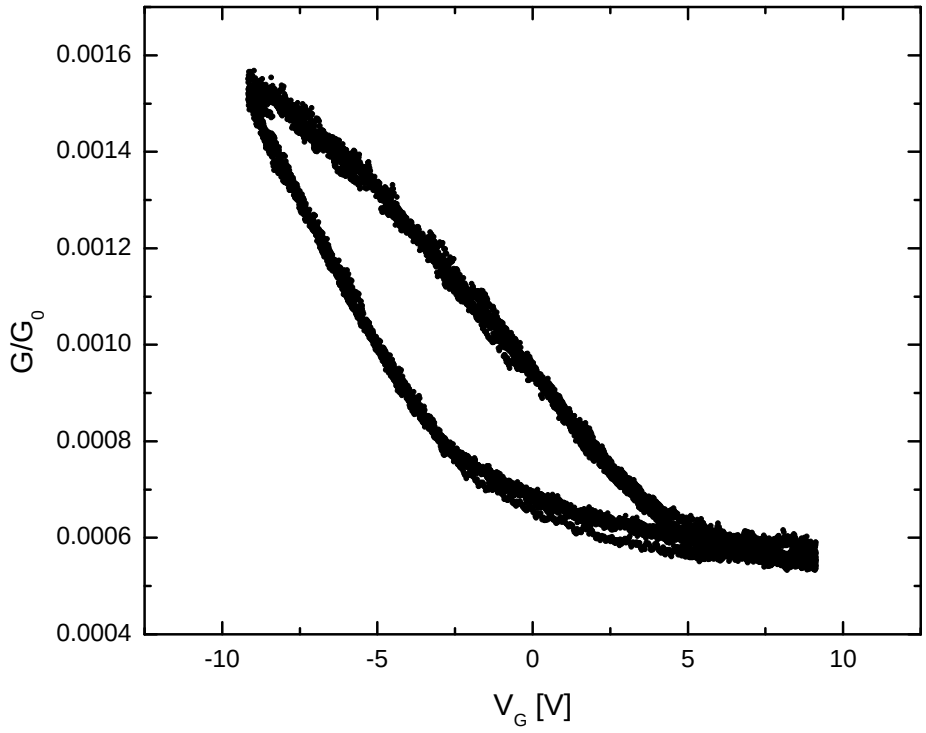

Figure 17: The conductance of the sample AFP11NT02 with Scandium electrodes as a function of the gate voltage V_G. V_{sd} =100 mV, $G_0 = 4e^2/h$. The direction of the gate scanning in the measurement was counter clockwise in this graph.

4.3.2 Carbon nanotube memory device

One of the possible applications for CNT devices is their use as a memory device. The memory devices used in computers require that each bit can be read and written fast. The SWCNT devices we have measured have the ability to store one bit per device. Because of the charge traps explained before the SWCNT device contains two different conductance states when the applied gate voltage is zero. The high and low conductance states can be named 1 and 0 respectively. The states can be changed with either positive or negative voltage pulse and the value of the bit can be read by measuring the conductance of the tube.

The final measurement in our study was the gate pulsing of the CNT device. The idea was to apply a relatively fast square pulse to the gate and use that to change to conductance state of the device. Peak to peak voltage of $6\ \mathrm{V}$ and pulse length of $12\ \mathrm{s}$ was used to apply both positive and negative pulses. Pulsing was done with Agilent 33220A $20\ \mathrm{MHz}$ Function/Arbitrary Waveform Generator connected to the gate. The used pulse generator was programmable and could be used to produce custom shaped pulses. Pulsing and the corresponding change in the conductance can be seen in figure 18.

A few of the best devices with palladium electrodes were measured. The pulsing response for the devices was generally good. The on and off state looked usually stable but the the difference between the states was quite small as can be seen from figure 18.

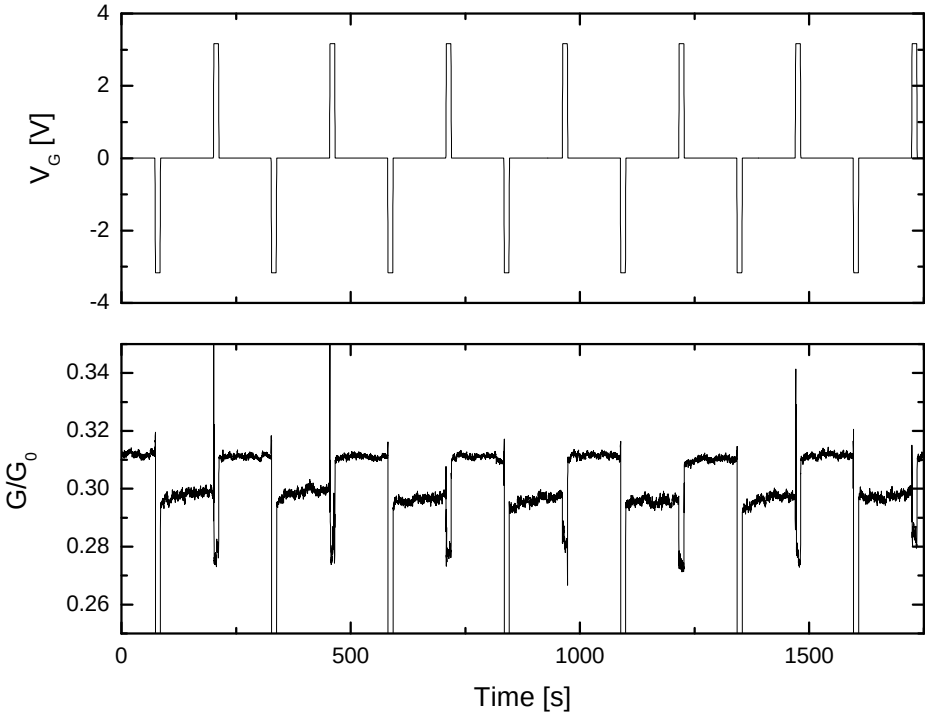

Figure 18: Pulsing of the sample AFP03NT05 with palladium electrodes. The pulse length was T_p =12 s and the time between pulses was T =114 s. The two different values of conductance can easily be seen but the difference between them is not large.

5 Conclusions

In this work we manufactured field-effect transistors from single-walled azafullerene dimer-filled carbon nanotubes. The devices were manufactured on top of a Si chip with SiO_2 as an insulating layer between the device and the Si gate electrode. The electrodes used to connect the SWCNT peapod device to the measuring setup were made of palladium and scandium. The electrical properties of the manufactured devices were measured. All of the measured devices were found to be semiconducting with a small energy gap and a hysteresis effect typical to CNT FETs was also found. The conduction channels of the measured devices opened up with a negative gate voltage which suggests that holes are the main charge carriers in the peapod devices making them p-type FETs. The conductance of the samples made with scandium electrodes was significantly lower possibly due to a formation of scandium oxide on top of the scandium electrodes. In addition to oxidation problems the graphite crucibiles used to evaporate scandium may have contaminated the evaporated material with scandium-graphite. The quality of the scandium electrodes needs to be improved in future and one possible solution is to change the graphite crucible to a crucible made of aluminium oxide and perform the evaporation in UHV evaporator.

The azafullerene dimers inside the SWCNTs did not have a large effect on the overall transfer characteristics and the ability to work as a nano scale memory device. The measured azafullerene peapods were found out to have p-type charge transfer characteristics with both palladium and scandium as an electrode material. More measurements are needed to verify this result especially because there have been measurements showing that a combination of gold electrodes with azafullerene peapods and scandium electrodes with pristine CNTs produce devices with n-type behaviour.

References

[1] T. KANEKO, Y. LI, S. NISHIGAKI AND R. HATAKEYAMA. *Azafullerene encapsulated single-walled carbon nanotubes with n-type electrical transport property*. Journal of the American Chemical Society **130**, 2714 (2008).

[2] Z. ZHANG, X. LIANG, S. WANG, K. YAO, Y. HU, Y. ZHU, Q. CHEN, W. ZHOU, Y. LI, Y. YAO, J. ZHANG AND L.-M. PENG. *Doping-free fabrication of carbon nanotube based ballistic cmos devices and circuits*. Nano Letters **7**, 3603 (2007).

[3] Z. Y. ZHANG, S. WANG, L. DING, X. L. LIANG, H. L. XU, J. SHEN, Q. CHEN, R. L. CUI, Y. LI AND L.-M. PENG. *High-performance n-type carbon nanotube field-effect transistors with estimated sub-10-ps gate delay*. Applied Physics Letters **92**, 133117 (2008).

[4] H. W. KROTO, J. R. HEATH, S. C. O'BRIEN, R. F. CURL AND R. E. SMALLEY. *C_{60}: Buckminsterfullerene*. Nature **318**, 162 (1985).

[5] S. IIJIMA. *Helical microtubules of graphitic carbon*. Nature **354**, 56 (1991).

[6] T. RUECKES, K. KIM, E. JOSELEVICH, G. Y. TSENG, C.-L. CHEUNG AND C. M. LIEBER. *Carbon nanotube-based nonvolatile random access memory for molecular computing*. Science **289**, 94 (2000).

[7] S. J. TANS, A. R. M. VERSCHUEREN AND C. DEKKER. *Room-temperature transistor based on a single carbon nanotube*. Nature **393**, 49 (1998).

[8] R. MARTEL, T. SCHMIDT, H. R. SHEA, T. HERTEL AND P. AVOURIS. *Single- and multi-wall carbon nanotube field-effect transistors*. Applied Physics Letters **73**, 2447 (1998).

[9] A. JORIO, M. S. DRESSELHAUS AND G. DRESSELHAUS, editors. *Carbon Nanotubes Advanced Topics in the Synthesis, Structure, Properties and Applications*. Springer, 1st edition (2008). ISBN 978-3-540-72864-1.

[10] A. JAVEY, M. SHIM AND H. DAI. *Electrical properties and devices of large-diameter single-walled carbon nanotubes*. Applied Physics Letters **80**, 1064 (2002).

[11] C. T. WHITE AND T. N. TODOROV. *Nanotubes go ballistic*. Nature **411**, 649 (2001).

[12] M. S. FUHRER, B. M. KIM, T. DÜRKOP AND T. BRINTLINGER. *High-mobility nanotube transistor memory*. Nano Letters **2**, 755 (2002).

[13] M. RINKIÖ, A. JOHANSSON, M. Y. ZAVODCHIKOVA, J. J. TOPPARI, A. G. NASIBULIN, E. I. KAUPPINEN AND P. TÖRMÄ. *High-yield of memory elements from carbon nanotube field-effect transistors with atomic layer deposited gate dielectric*. New J. Phys. **10**, 103019 (2008).

[14] Q. CAO, S.-H. HUR, Z.-T. ZHU, Y. SUN, C. WANG, M. A. MEITL, M. SHIM AND J. A. ROGERS. *Highly Bendable, Transparent Thin-Film Transistors That Use Carbon-Nanotube-Based Conductors and Semiconductors with Elastomeric Dielectrics*. Advanced Materials **18**, 304 (2006).

[15] H. SHIMODA, B. GAO, X. P. TANG, A. KLEINHAMMES, L. FLEMING, Y. WU AND O. ZHOU. *Lithium Intercalation into Opened Single-Wall Carbon Nanotubes: Storage Capacity and Electronic Properties*. Physical Review Letters **88**, 015502 (2002).

[16] C. KIM, Y. J. KIM, YOONG AM KIM, NEWAUTHOR9, K. C. PARK, M. ENDO AND M. S. DRESSELHAUS. *High performance of cup-stacked-type carbon nanotubes as a Pt–Ru catalyst support for fuel cell applications*. Journal of Applied Physics **96**, 5903 (2004).

[17] K. KORDÁS, G. TÓTH, P. MOILANEN, M. KUMPUMÄKI, J. VÄHÄKANGAS AND A. UUSIMÄKI. *Chip cooling with integrated*

carbon nanotube microfin architectures. Applied Physics Letters **90**, 123105 (2007).

[18] R. H. BAUGHMAN, A. A. ZAKHIDOV AND W. A. DE HEER. *Carbon Nanotubes–the Route Toward Applications*. Science **297**, 787 (2002).

[19] J. SUHR, W. ZHANG, P. M. AJAYAN AND N. A. KORATKAR. *Temperature-Activated Interfacial Friction Damping in Carbon Nanotube Polymer Composites*. Nano Letters **6**, 219 (2006).

[20] M. ENDO, S. KOYAMA, Y. MATSUDA, T. HAYASHI AND Y.-A. KIM. *Thrombogenicity and Blood Coagulation of a Microcatheter Prepared from Carbon Nanotube-Nylon-Based Composite*. Nano Letters **5**, 101 (2005).

[21] P. QI, O. VERMESH, M. GRECU, A. JAVEY, Q. WANG AND H. DAI. *Toward Large Arrays of Multiplex Functionalized Carbon Nanotube Sensors for Highly Sensitive and Selective Molecular Detection*. Nano Letters **3**, 347 (2003).

[22] W. B. CHOI, D. S. CHUNG, J. H. KANG, H. Y. KIM, Y. W. JIN, I. T. HAN, Y. H. LEE, J. E. JUNG, N. S. LEE, G. S. PARK AND J. M. KIM. *Fully sealed, high-brightness carbon-nanotube field-emission display*. Applied Physics Letters **75**, 3129 (1999).

[23] D. A. HELLER, E. S. JENG, T.-K. YEUNG, B. M. MARTINEZ, A. E. MOLL, J. B. GASTALA AND M. S. STRANO. *Optical Detection of DNA Conformational Polymorphism on Single-Walled Carbon Nanotubes*. Science **311**, 508 (2006).

[24] D. S. BETHUNE, C. H. KLANG, M. S. DE VRIES, G. GORMAN, R. SAVOY, J. VAZQUEZ AND R. BEYERS. *Cobalt-catalysed growth of carbon nanotubes with single-atomic-layer walls*. Nature **363**, 605 (1993).

[25] M. WILSON, K. KANNANGARA, G. SMITH AND M. SIMMONS. *Nanotechnology: Basic Science and Emerging Technologies*. CRC Press (2002). ISBN 1-58488-339-1.

[26] B. W. SMITH, M. MONTHIOUX AND D. E. LUZZI. *Encapsulated C_{60} in carbon nanotubes*. Nature **396**, 323 (1998).

[27] M. S. DRESSELHAUS, G. DRESSELHAUS AND P. AVOURIS, editors. *Carbon Nanotubes Synthesis, Structure, Properties, and Applications*. Springer (2001). ISBN 3-540-41086-4.

[28] K. HIRAHARA, K. SUENAGA, S. BANDOW, H. KATO, T. OKAZAKI, H. SHINOHARA AND S. IIJIMA. *Dimensional metallofullerene crystal generated inside single-walled carbon nanotubes*. Physical Review Letters **85**, 5384 (2000).

[29] B. W. SMITH AND D. E. LUZZI. *Formation mechanism of fullerene peapods and coaxial tubes: a path to large scale synthesis*. Chemical Physics Letters **321**, 169 (2000).

[30] P. AVOURIS. *Molecular electronics with carbon nanotubes*. Accounts of chemical research **35**, 1026 (2002).

[31] J. W. G. WILDÖER, L. C. VENEMA, A. G. RINZLER, R. E. SMALLEY AND C. DEKKER. *Electronic structure of atomically resolved carbon nanotubes*. Nature **391**, 59 (1998).

[32] A. JORIO, R. SAITO, J. H. HAFNER, C. M. LIEBER, M. HUNTER, T. MCCLURE, G. DRESSELHAUS AND M. S. DRESSELHAUS. *Structural (n,m) Determination of Isolated Single-Wall Carbon Nanotubes by Resonant Raman Scattering*. Physical Review Letters **86**, 1118 (2001).

[33] S. HEINZE, J. TERSOFF, R. MARTEL, V. DERYCKE, J. APPENZELLER AND P. AVOURIS. *Carbon nanotubes as schottky barrier transistors*. Physical Review Letters **89**, 106801 (2002).

[34] A. JAVEY, J. GUO, Q. WANG, M. LUNDSTROM AND H. DAI. *Ballistic carbon nanotube field-effect transistors*. Nature **424**, 654 (2003).

[35] Y. YAISH, J.-Y. PARK, S. ROSENBLATT, V. SAZONOVA, M. BRINK AND P. L. MCEUEN. *Electrical Nanoprobing of Semiconducting Carbon Nanotubes Using an Atomic Force Microscope*. Physical Review Letters **92**, 046401 (2004).

[36] A. ROBERT-PEILLARD AND S. V. ROTKIN. *Modeling hysteresis phenomena in nanotube field-effect transistors*. IEEE Transactions on Nanotechnology **4**, 284 (2005).

[37] W. KIM, A. JAVEY, O. VERMESH, Q. WANG, Y. LI AND H. DAI. *Hysteresis caused by water molecules in carbon nanotube field-effect transistors*. Nano Letters **3**, 193 (2003).

[38] M. FREITAG, A. T. JOHNSON, S. V. KALININ AND D. A. BONNELL. *Role of Single Defects in Electronic Transport through Carbon Nanotube Field-Effect Transistors*. Physical Review Letters **89**, 216801 (2002).

[39] J. PARK. *Electrically tunable defects in metallic single-walled carbon nanotubes*. Applied Physics Letters **90**, 023112 (2007).

[40] H. KUZMANY, W. PLANK, J. WINTER, O. DUBAY, N. TAGMATARCHIS AND K. PRASSIDES. *Raman spectrum and stability of* $(c_{59}n)_2$. Physical Review B **60**, 1005 (1999).

[41] D. H. LOESCHER, G. E. PIKE AND J. A. BORDERS. *Oxidation of Scandium*. Journal of Vacuum Science and Technology **9**, 159 (1972).

[42] S. A. MCGILL, S. G. RAO, P. MANANDHAR, P. XIONG AND S. HONG. *High-performance, hysteresis-free carbon nanotube field-effect transistors via directed assembly*. Applied Physics Letters **89** (2006).